

Modular organization of the brainstem noradrenaline system coordinates opposing learning states

Akira Uematsu^{1,9} , Bao Zhen Tan^{1,9}, Edgar A Ycu¹, Jessica Sulkes Cuevas^{1,2}, Jenny Koivumaa¹, Felix Junyent³, Eric J Kremer³, Ilana B Witten⁴, Karl Deisseroth⁵⁻⁷ & Joshua P Johansen^{1,2,8} 

Noradrenaline modulates global brain states and diverse behaviors through what is traditionally believed to be a homogeneous cell population in the brainstem locus coeruleus (LC). However, it is unclear how LC coordinates disparate behavioral functions. We report a modular LC organization in rats, endowed with distinct neural projection patterns and coding properties for flexible specification of opposing behavioral learning states. LC projection mapping revealed functionally distinct cell modules with specific anatomical connectivity. An amygdala-projecting ensemble promoted aversive learning, while an independent medial prefrontal cortex-projecting ensemble extinguished aversive responses to enable flexible behavior. LC neurons displayed context-dependent inter-relationships, with moderate, discrete activation of distinct cell populations by fear or safety cues and robust, global recruitment of most cells by strong aversive stimuli. These results demonstrate a modular organization in LC in which combinatorial activation modes are coordinated with projection- and behavior-specific cell populations, enabling adaptive tuning of emotional responding and behavioral flexibility.

The neuromodulator noradrenaline participates in a broad range of functions, including arousal, stress, emotional learning, behavioral flexibility, decision-making and perception, and is an important therapeutic target for anxiety and mood disorders¹⁻⁷. Neurons in the brainstem LC are the major source of noradrenaline to the forebrain, through what was traditionally thought to comprise a homogeneous population of LC noradrenaline neurons projecting to many brain regions through highly ramified axonal arborization and coordinated, uniform responses to sensory stimuli⁸⁻¹². However, some studies have suggested heterogeneity in LC cells, including anatomical experiments indicating that LC neurons exhibit specificity in their efferent connectivity with other brain regions^{6,8,10,13-17}. How the firing properties and anatomical organization of LC neurons coordinate the diverse functions of noradrenaline and whether the LC functions homo- or heterogeneously during learning and behavior remain critical open questions.

Here we explored these questions by focusing on two important roles of the LC in mediating emotional learning and behavioral flexibility. Pharmacology studies indicate that adrenergic receptor (AR) activation in the amygdala regulates anxiety and emotional fear learning¹⁸⁻²⁰ (also termed ‘threat conditioning’²¹; see Online Methods), in which an auditory cue (conditioned stimulus, CS) predicts the occurrence of an aversive outcome (unconditioned stimulus, US), and animals exhibit measurable behavioral and visceral responses upon auditory CS presentation following learning^{22,23}. Furthermore, noradrenaline levels increase in the amygdala during fear conditioning²⁴.

By contrast, adrenergic receptor activation in the medial prefrontal cortex (mPFC) is required for flexible reversal learning and fear extinction learning^{5,25}, a process through which emotional fear responses are overridden to facilitate adaptive, flexible behavior when the auditory CS is presented repeatedly without shock. Moreover, noradrenaline levels are enhanced in mPFC following extinction learning²⁶. The differential effects of noradrenaline in these brain regions could arise from a homogeneous population of LC neurons or from unique populations of LC noradrenaline neurons with specific modular functionality and anatomical connectivity with the amygdala or mPFC.

Using a comprehensive technical approach to study the anatomical, functional and neurophysiological properties of the LC, we examined how the circuit and neural-coding features of this neuromodulatory system regulate both aversive emotional learning and behavioral flexibility. Our findings reveal a modular organization in the LC in which emergent functional properties arise through the combination of individual organizational elements, including functional modularity, specific efferent connectivity and combinatorial response features. This organization may allow for dynamic control of the level and spatial targeting and the specificity of noradrenaline release in response to changing adaptive demands, and it functions to coordinate fear and extinction learning. The results suggest a revised view of the functional organization of this neuromodulatory system, with implications for understanding psychiatric disorders associated with their dysfunction.

¹RIKEN Brain Science Institute, Laboratory for Neural Circuitry of Memory, Wako, Japan. ²Department of Life Sciences, Graduate School of Arts and Sciences, University of Tokyo, Tokyo, Japan. ³Institut de Génétique Moléculaire de Montpellier, Montpellier, France. ⁴Princeton Neuroscience Institute and Department of Psychology, Princeton, New Jersey, USA. ⁵Bioengineering Department, Stanford University, Stanford, California, USA. ⁶CNC Program, Stanford University, Stanford, California, USA. ⁷Howard Hughes Medical Institute, Stanford University, Stanford, California, USA. ⁸RIKEN BSI-Kao Collaboration Center, Wako, Japan. ⁹These authors contributed equally to this work. Correspondence should be addressed to J.P.J. (jjohans@brain.riken.jp) or A.U. (akirauematsu0104@gmail.com).

Received 5 May; accepted 17 August; published online 18 September 2017; doi:10.1038/nn.4642

RESULTS

Involvement of LC noradrenaline neurons in fear and extinction learning

To examine whether LC noradrenaline neurons are functionally important for fear and extinction learning, we injected adeno-associated viral (AAV) vectors carrying a construct that encodes the inhibitory opsin archaerhodopsin T (ArchT)²⁷ fused with GFP under the control of Cre-recombinase into the LC of tyrosine hydroxylase (TH)-Cre-recombinase rats²⁸ to inhibit neural activity in this cell population during the different learning tasks. We confirmed that the expression of ArchT was specific to TH⁺ neurons in the LC (>95%; **Fig. 1a**) and verified optical inhibition of shock-evoked responding in these cells (**Fig. 1b**). We first asked whether the activity of LC noradrenaline neurons specifically during the tone or shock period was important for fear memory formation. Using chronically implanted fiberoptic cannulae (**Fig. 1c**) attached to orange lasers, we bilaterally inhibited LC noradrenaline neurons during either the tone or shock period (or for equivalent time periods during the intertrial interval; referred to as offset groups) of fear conditioning. We found that inhibition during the shock, but not tone, period of training moderately reduced auditory fear learning when tested later in a novel context (**Fig. 1d–f**). We did not see effects on freezing during the training period, likely because context-induced freezing predominated, and during training this response is insensitive to noradrenaline manipulations^{29,30}. Next, we tested whether LC noradrenaline neuronal activity during the tone CS or shock-omission period was important for extinction learning. Optical inhibition of LC noradrenaline activity during the tone CS or shock-omission period did not impair extinction during the learning session (**Fig. 1g–i**), but freezing responses partially recovered the next day in animals that had received inhibition during the tone CS period (**Fig. 1h**). Thus, using global inhibition of LC noradrenaline neurons, these results demonstrate that aversive activation of LC noradrenaline neurons participates in fear learning, while LC noradrenaline activity during the auditory CS period is important for fear extinction.

Heterogeneous response properties in LC neurons during different forms of learning

To determine whether LC noradrenaline neurons respond homo- or heterogeneously during fear and extinction learning, we analyzed their neural coding properties using chronically implanted drivable stereotrodes and tetrodes in the LC to record extracellular spiking activity from single neurons in behaving animals during and after fear and extinction learning and also after overtraining ($n = 61$ LC neurons from 9 rats; **Supplementary Fig. 1a**). We first examined fear and extinction learning-induced changes in auditory CS-evoked responses (**Fig. 2a–g**). To validate that the same LC cells were recorded throughout fear and extinction learning, we correlated the average waveforms across pretraining, fear conditioning and extinction, and we only included cells with >0.95 correlations across all sessions (see **Supplementary Fig. 1b** and Online Methods for details of sorting). We found that discrete populations of LC neurons were differentially regulated following fear and extinction learning. One population of neurons responded more to auditory CSs following fear learning (fear neurons; **Fig. 2b,d,f,g**), and some of these continued to respond during extinction learning (fear + extinction neurons; **Fig. 2d,f,g**), consistent with previous reports^{31–33}. This was also apparent after overtraining, as some of the recorded cells responded to shock predictive cues (**Supplementary Fig. 1c–g**). By contrast, another population did not change their auditory CS response with fear conditioning but exhibited increased auditory-evoked responding during later extinction learning (extinction neurons; **Fig. 2c,d,f,g**). A third population

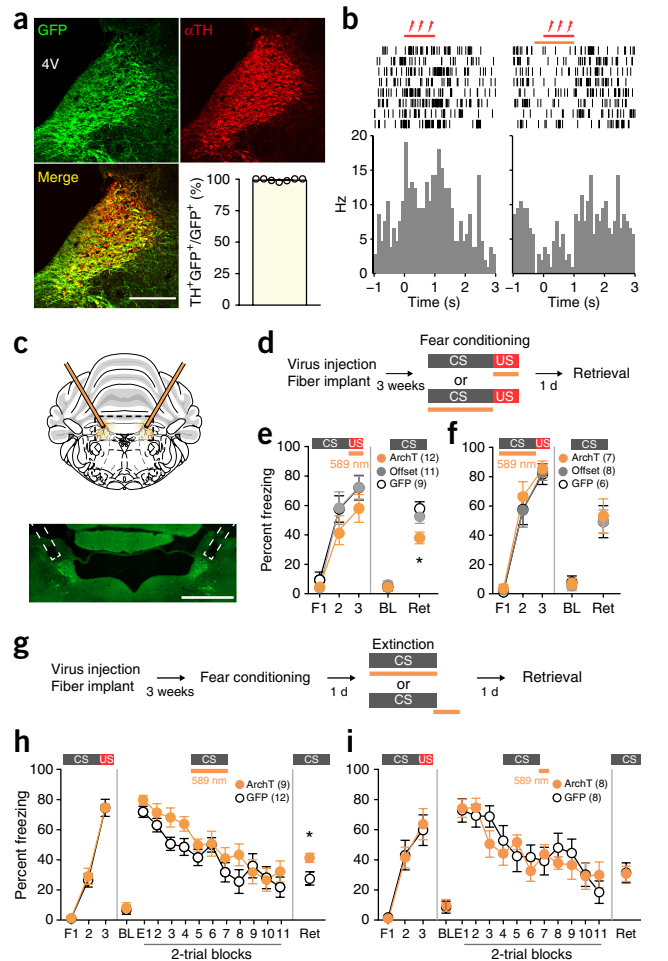


Figure 1 LC noradrenaline neural activity is necessary for fear and extinction memory formation at specific time points. **(a)** Representative images showing expression of ArchT-GFP (green) in TH⁺ neurons (red) in the LC of TH-Cre rats (yellow, overlay; scale bar, 200 μ m). Graph shows percentage of GFP⁺ cells co-labeled for TH. **(b)** Perievent time histograms of an example LC neuron recorded in an awake, behaving ArchT⁺ TH-Cre rat, showing aversive shock-evoked firing rate responses before, during (red bar with lightning symbols) and after shock presentation without (left) and with (right) laser illumination (orange bar). Shock onset was at 0 s (duration = 1 s). **(c)** Schematic of fiber implantation (top) and representative image of LC (bottom) with fiber track outlined in white. Scale bar, 1 mm. **(d)** Experimental design of optogenetic manipulation during fear conditioning. **(e,f)** Optogenetic inactivation of LC noradrenaline neurons during **(e)** the shock US period (retrieval: $F_{2,28} = 5.46$, $P = 0.01$, one-way ANOVA; conditioning: interaction, $F_{4,58} = 0.39$, $P = 0.81$; main effect of group, $F_{2,29} = 2.08$, $P = 0.14$, two-way repeated-measures (RM) ANOVA) but **(f)** not the auditory CS period (retrieval: $F_{2,18} = 0.050$, $P = 0.95$, one-way ANOVA; conditioning: interaction, $F_{4,36} = 0.13$, $P = 0.97$; main effect of group, $F_{2,18} = 0.29$, $P = 0.76$, two-way RM ANOVA) reduced fear-memory formation, measured as freezing responses 24 h after learning. F, fear conditioning; BL, baseline; ret, retrieval. **(g)** Experimental design of optogenetic manipulation during fear extinction. **(h,i)** Inactivation during the tone CS period but not during the shock-omission period of extinction reduced consolidation of extinction memories measured 24 h after extinction (**h**: unpaired t test, $t_{19} = 2.23$, $P = 0.04$; **i**: $t_{14} = 0.08$, $P = 0.95$) but not within-session extinction (**h**: interaction $F_{10,200} = 1.08$, $P = 0.37$; main effect of group, $F_{1,20} = 1.77$, $P = 0.20$; **i**: interaction, $F_{10,140} = 1.32$, $P = 0.23$; main effect of group, $F_{1,14} = 0.065$, $P = 0.80$, two way RM ANOVA). E, extinction. Data represent mean \pm s.e.m.; numbers in parentheses represent the number of samples; * $P < 0.05$ from Newman-Keuls *post hoc* tests.

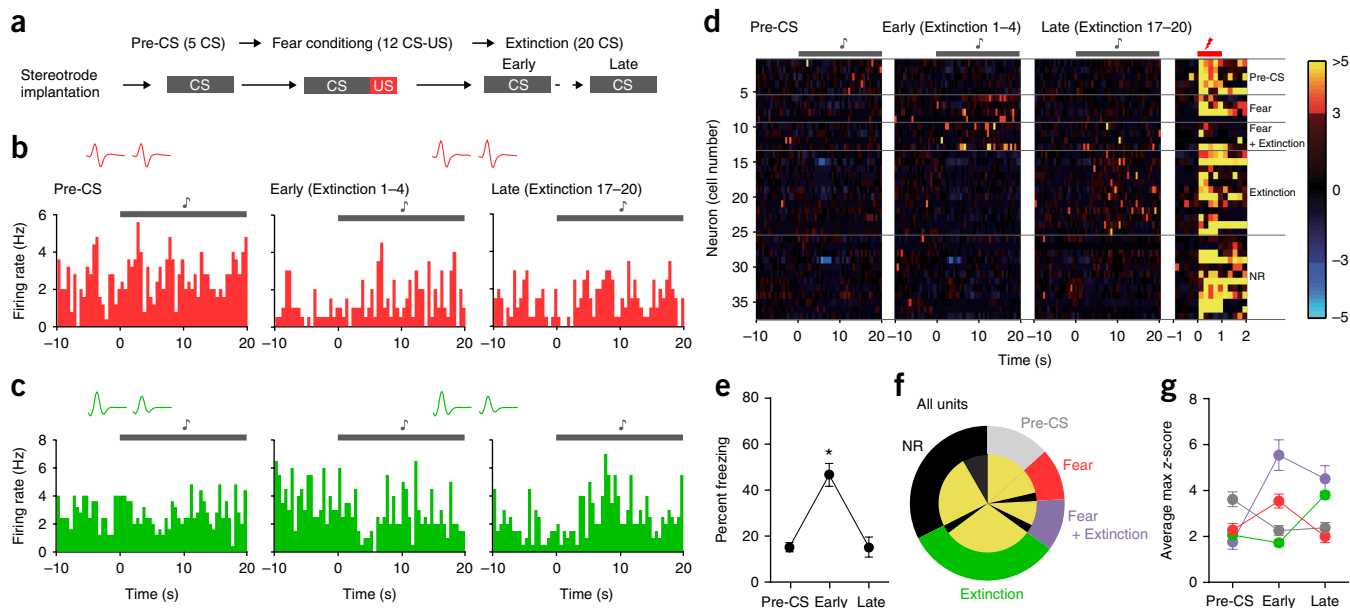


Figure 2 Context-dependent global or discrete coding in LC neurons in response to aversive shocks or state-specific sensory cues. **(a)** Schematic of experimental design. Pre-CS, pretraining; early, early extinction (a high fear period); late, late extinction (a period during which fear responses are reduced; see **e**). **(b,c)** Perievent time histogram showing auditory-evoked firing rate (gray bar, auditory CS period) during pre-CS (left), early (middle) and late (right) extinction in two example fear **(b)** and extinction **(c)** LC neurons. CS onset is at 0 s. Bin size, 500 ms. **(d)** Heat plot showing auditory CS-evoked responses of all LC neuron recorded during pre-CS (left), early (middle) and late (right) extinction arranged vertically according to response type. Tone CS onset (top gray bar) is at 0 s. Bin size, 500 ms. Far right heat plot shows shock-evoked responses in the same neurons (shock period in orange above; bin size, 200 ms; NR, nonresponsive). Color code bar (far right) indicates z-score. **(e)** Behavioral freezing responses during pre-CS and after fear conditioning during early and late extinction for all animals in which cells were recorded ($F_{2,16} = 29.27$, $P < 0.001$, one-way RM ANOVA; * $P < 0.05$, Newman Keuls *post hoc* test, $n = 9$). **(f)** Proportion of all LC cells recorded across all tasks ($n = 37$) that were classified as pre-CS (gray, $n = 5$, 14%), fear (red, $n = 4$, 11%), fear + extinction (purple, $n = 4$, 11%), extinction (blue, $n = 12$, 32%) or nonresponsive (black, 32%). Yellow area shows the proportion of shock-responsive cells in each cell classification. **(g)** Population averaged auditory CS-evoked response analysis (significant interaction, $F_{6,42} = 24.6$, $P < 0.0001$, two-way RM ANOVA; Newman-Keuls *post hoc* test) at pre-CS, early and late extinction for each cell type, showing significant enhancement of auditory-evoked responding during pre-CS training compared with early and late (in pre-CS cells, $P < 0.01$ for both), significantly increased responses at early compared with pre-CS training and late extinction periods (in fear cells, $P < 0.01$), significantly enhanced responding during early and late extinction compared with pre-CS (in fear + extinction cells, $P < 0.0001$) and significantly increased tone CS responding at late compared with early extinction and with pre-CS (in extinction cells, $P < 0.0001$). Data represent mean \pm s.e.m.

responded more to the auditory CS upon initial exposure and then exhibited a reduction in auditory responding after the initial pre-training, tone CS-alone session (**Fig. 2d,f,g**). This relatively weak, heterogeneous responding of LC neurons to novel auditory cues was likely due to the low decibel level of the auditory stimulus, resulting in little behavioral orienting. We next examined baseline firing rate changes in the LC neurons we recorded and found no significant change across the different task conditions when analyzing all LC neurons (20-s baseline: $P = 0.37$; 60-s baseline: $P = 0.37$) or the individual cell populations (20-s baseline: $P = 0.67$, 60-s baseline: $P = 0.56$; **Supplementary Fig. 2a–d**). Although all LC neurons are presumed to be noradrenergic in the rat LC³⁴, we used an optogenetic identification approach (**Supplementary Fig. 2e,f**) in some of the cells we recorded to validate our findings in identified noradrenaline neurons. Using this technique, a similar pattern of results was apparent (**Supplementary Fig. 2g,h**). Notably, using this optogenetic identification approach, we found a subpopulation of LC noradrenaline neurons with higher baseline firing rates than has been reported previously (**Supplementary Fig. 3a–h**).

These results on heterogeneous and learning-state-dependent response properties of LC neurons are inconsistent with previous reports of homogeneous responses to sensory stimuli, particularly to those that are very salient^{1,3}. One possibility is that LC neurons have different response modes to sensory predictive cues and more salient, primary aversive stimuli. To test this, we examined whether LC

neurons exhibited homo- or heterogeneity in their responses to shock USs occurring during fear conditioning. Unexpectedly, we found that, despite their selectivity to sensory cues of different adaptive value, fear and extinction neurons did not differ in their shock responsiveness (**Supplementary Fig. 4a**). Furthermore, shock USs activated a significantly larger proportion of cells compared with the proportion of cells activated by the auditory CS during the pre-extinction, early extinction or late extinction periods, as well as after overtraining ($P = 0.0001$; **Fig. 2f** and **Supplementary Figs. 1e–g** and **4b**). Finally, shocks evoked a significantly larger response in LC neurons than the maximal response of sensory predictive cues presented after learning ($P = 0.0001$; **Fig. 2d** and **Supplementary Fig. 4c**). Together, the physiology data demonstrate that LC neurons exhibit distinct response modes: strong, global activation in response to more intensely aversive noxious stimuli and more moderate, discrete, dynamic responses to sensory predictive cues as environmental contingencies change during extinction.

Behavioral-state-dependent recruitment of distinct amygdala- or mPFC-projecting LC noradrenaline cell populations

Based on the findings that different populations of LC noradrenaline neurons are engaged during high or low fear states, we next asked whether anatomically distinct populations of noradrenaline neurons were recruited during early and late extinction. Drawing upon previous work showing that specific populations of LC neurons project to

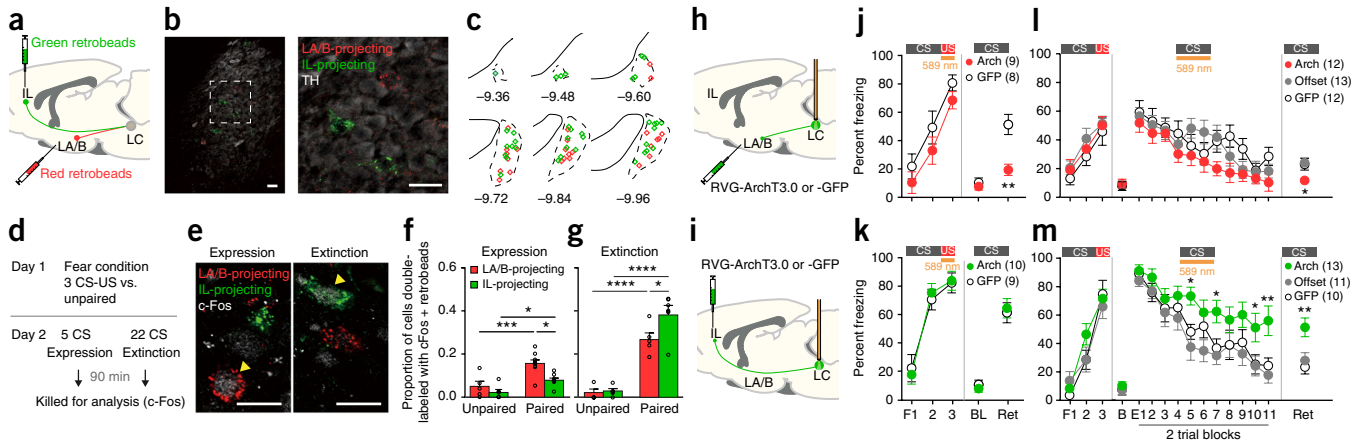


Figure 3 Projection-specific functional heterogeneity of LC noradrenaline neurons. **(a)** Schematic of red and green retrobead injections into amygdala and IL. **(b)** Representative image of retrobead labeling in the LC (red from LA/B, green from IL) after dual injections. TH immunostaining pseudocolored in gray. Right, close-up of white-outlined area in left image. **(c)** Reconstruction of LA/B- and IL-projecting neurons in and around the LC of retrobead injected animals. No cells were detected outside the LC. **(d)** Experimental design of c-Fos experiments. Retrobeads were injected 7–10 d before experiments. **(e)** Representative images of c-Fos expression (gray) in LA/B-projecting (red) and IL-projecting (green) neurons following fear-inducing tone CS presentation (expression, left) and after extinction (right). Arrowheads denote double-labeled cells. **(f,g)** Proportions of retrobead-labeled cells that were also c-Fos⁺ in LA/B- and IL-projecting cells in animals that had received paired CS–US training or unpaired controls. Dots represent individual animal data points. **(f)** c-Fos activity was increased in LA/B-projecting LC neurons ($n = 9$ animals) following exposure to fear-inducing auditory CSs compared with unpaired controls ($n = 5$) and IL-projecting cells ($n = 8$). IL-projecting cells in unpaired control, $n = 6$. Significant main effect of training, $F_{1,24} = 25.46$, $P < 0.0001$; main effect of group, $F_{1,24} = 10.80$, $P = 0.0031$; two-way ANOVA followed by Bonferroni *post hoc* test. **(g)** c-Fos activity was significantly increased in IL-projecting LC neurons (paired, $n = 6$) compared with LA/B-projecting LC neurons (paired $n = 5$) after extinction, and both increased relative to their unpaired controls (IL-projecting $n = 5$, LA/B-projecting $n = 4$). Significant main effect of training, $F_{1,16} = 100.50$, $P < 0.0001$; main effect of group, $F_{1,16} = 4.64$, $P = 0.047$, two-way ANOVA followed by Bonferroni *post hoc* test. **(h,i)** Schematics of RVΔG-eArchT3.0-EGFP or RVΔG-EGFP injection and fiber implantation for optogenetic manipulation of projection-specific subpopulations. **(j,k)** Inactivation of LA/B- or IL-projecting neurons had no effect on conditioning (**j**: interaction, $F_{2,30} = 0.070$, $P = 0.93$; main effect of group, $F_{1,15} = 2.28$, $P = 0.15$; **k**: interaction, $F_{2,34} = 0.32$, $P = 0.74$, two-way RM ANOVA) but reduced memory formation measured during retrieval. (**j**: $t_{15} = 4.05$, $P = 0.0011$; **k**: $t_{17} = 0.32$, $P = 0.95$, Student's *t* test). **(l,m)** Inactivation of LA/B-projecting neurons did not affect within-session extinction ($F_{20,350} = 1.08$, $P = 0.36$; main effect of group, $F_{2,35} = 2.15$, $P = 0.13$, two-way RM ANOVA) but facilitated later retrieval of extinction memory interaction ($F_{2,34} = 4.27$, $P = 0.022$, one-way ANOVA). Inactivation of IL-projecting neurons reduced within-session extinction (interaction, $F_{20,300} = 1.70$, $P = 0.032$, two-way RM ANOVA) and later retrieval ($F_{2,31} = 6.78$, $P = 0.0036$, one-way ANOVA). Newman-Keuls test was used for *post hoc* analyses. * $P < 0.05$, ** $P < 0.01$, *** $P < 0.001$, **** $P < 0.0001$. Data represent mean \pm s.e.m.; numbers in parentheses represent sample sizes. All scale bars, 20 μ m.

distinct brain regions^{6,8,13} and the importance of noradrenaline in the amygdala and mPFC for fear or extinction learning^{5,19,20,25}, we first examined whether different populations of LC noradrenaline neurons project to these regions. To test this question, we injected different colored retrobeads into the lateral and basal nuclei of the amygdala (LA/B) and the infralimbic region of the mPFC (IL, an mPFC subregion particularly important for extinction) and examined their expression pattern and overlap in LC neurons (Fig. 3a,b). Injection of retrobeads or other tracers into LA/B or IL mostly labeled ipsilateral LC noradrenaline (TH⁺) neurons (100% of neurons retrogradely labeled from LA/B ($n = 3$ rats) and IL ($n = 3$) were TH⁺ using retrobeads; Fig. 3b). With double retrobead injections (Fig. 3b), we found very little overlap in the LC noradrenaline cells that project to the LA/B and IL (5% of LA/B projecting neurons overlapped with IL-projecting cells; 3.9% of IL-projecting cells overlap with LA/B-projecting cells). Notably, LA/B and IL projecting cells were intermixed in the LC and displayed no obvious topography in their organization (Fig. 3b,c). We validated this finding using combinations of other retrograde tracers (Supplementary Fig. 5a,b) and verified that co-injection of different tracers into the same location produced substantial overlap in LC neurons (Supplementary Fig. 5c). Finally, we also examined this in the mouse and found similarly non-overlapping amygdala and mPFC projecting LC noradrenaline cell populations (Supplementary Fig. 5d).

Next, we tested whether the balance of activity in these distinct LC cell populations shifted during fear (occurring early in extinction) and safety (occurring late in extinction) states, as we saw in the physiologically defined cell populations. To study this question, we used triple-label immunohistochemistry, combining the double retrograde tracing strategy described above and activity-dependent labeling of these cell populations using the immediate early gene *Fos* as a marker of activity (Fig. 3d,e). Following aversive learning, fear-inducing auditory CS presentation (which increased freezing levels relative to unpaired controls; Supplementary Fig. 6a) increased the number of c-Fos labeled LA/B-projecting neurons relative to IL-projecting cells (Fig. 3e,f). By contrast, following extinction learning (which produced reductions in freezing in the previously fear conditioned groups; Supplementary Fig. 6b), the balance of activity shifted, such that more IL-projecting neurons compared with LA/B-projecting neurons were c-Fos⁺ (Fig. 3e,g). However, both cell populations were significantly more activated than in controls, possibly reflecting the fact that the extinction session consists of an initial fear state followed by extinction learning (Fig. 3g). Consistent with our physiology data and with previous studies showing that many LC noradrenaline neurons respond to aversive stimuli (see refs. 1,3 for review), equal proportions of LA/B- and IL-projecting LC noradrenaline neurons were activated following fear learning (LA/B: 0.22 ± 0.05 , IL: 0.23 ± 0.04 ; $t_{10} = 0.07$, $P = 0.94$, unpaired *t* test). These data demonstrate

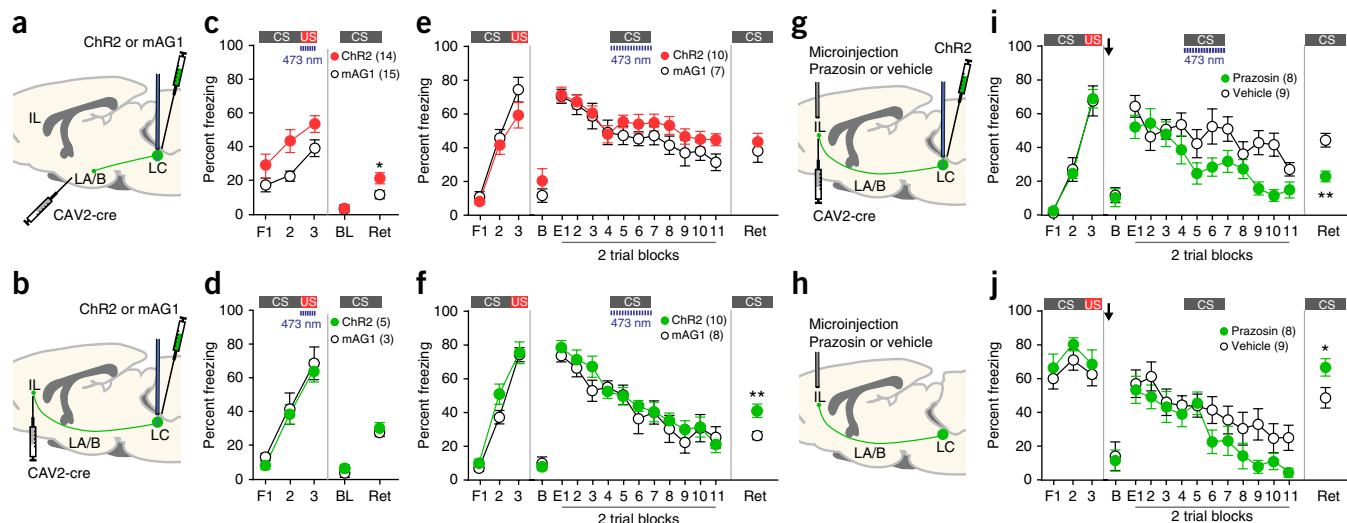


Figure 4 Optogenetic stimulation of amygdala or mPFC projecting cells. (a,b) Schematic of CAV2-Cre injection into LA/B or IL, combined with AAV-FLEX-ChR2-mAG1 or AAV-FLEX-mAG1 injection into LC. Optic fibers were located above LC. (c,d) 10-Hz stimulation of (c) LA/B-projecting but not (d) IL-projecting cells during weak US (0.3 mA) significantly increased fear learning (LA/B: conditioning: interaction $F_{2,54} = 0.53$, $P = 0.59$; main effect of group, $F_{1,27} = 8.36$, $P = 0.0075$, two-way RM ANOVA; retrieval: $t_{27} = 2.49$, $P = 0.019$, Student's t test; IL: conditioning: interaction, $F_{2,12} = 0.014$, $P = 0.98$; main effect of group, $F_{1,6} = 0.43$, $P = 0.54$, two-way RM ANOVA; retrieval: $t_6 = 0.57$, $P = 0.59$, Student's t test). (e,f) 5-Hz stimulation of (f) IL-projecting but not (e) LA/B-projecting neurons reduced long-term extinction memory (LA/B: within-session: interaction $F_{10, 150} = 0.67$, $P = 0.75$; main effect of group, $F_{1,15} = 1.72$, $P = 0.21$, two-way RM ANOVA; retention: $t_{15} = 0.65$, $P = 0.53$, Student's t test; IL: within-session: interaction, $F_{10, 160} = 0.71$, $P = 0.72$; main effect of group, $F_{1,16} = 0.40$, $P = 0.54$, two-way RM ANOVA; retention: $t_{16} = 2.96$, $P = 0.0093$, Student's t test). (g) Schematic of optostimulation of IL-projecting neurons combined with pharmacology (Prazosin or vehicle injected into IL). (h) Schematic of pharmacology-alone experiments. (i) Prazosin or vehicle was injected into IL 10 min before extinction session (black arrow). Prazosin microinjection into IL combined with 5-Hz optostimulation of IL-projecting LC neurons significantly decreased freezing relative to vehicle-treated animals during extinction learning and retrieval (within-session: interaction, $F_{10, 150} = 1.76$, $P = 0.072$; significant main effect of group, $F_{1,15} = 6.62$, $P = 0.021$, two-way RM ANOVA; retention: $t_{15} = 4.08$, $P = 0.0010$, Student's t test). (j) Prazosin microinjection without optostimulation significantly reduced long-term extinction memory (within-session: interaction, $F_{10, 150} = 1.20$, $P = 0.30$; main effect of group, $F_{1,15} = 2.19$, $P = 0.16$, two-way RM ANOVA; retention: $t_{15} = 2.22$, $P = 0.043$, Student's t test). * $P < 0.05$, ** $P < 0.01$. Data represent mean \pm s.e.m.; numbers in parentheses represent sample sizes.

that separate populations of LC noradrenaline neurons project to amygdala or mPFC and that these distinct cell populations can be differentially recruited by fear and safety states or be activated as an ensemble during fear learning.

Modularity of function in LC noradrenaline neurons

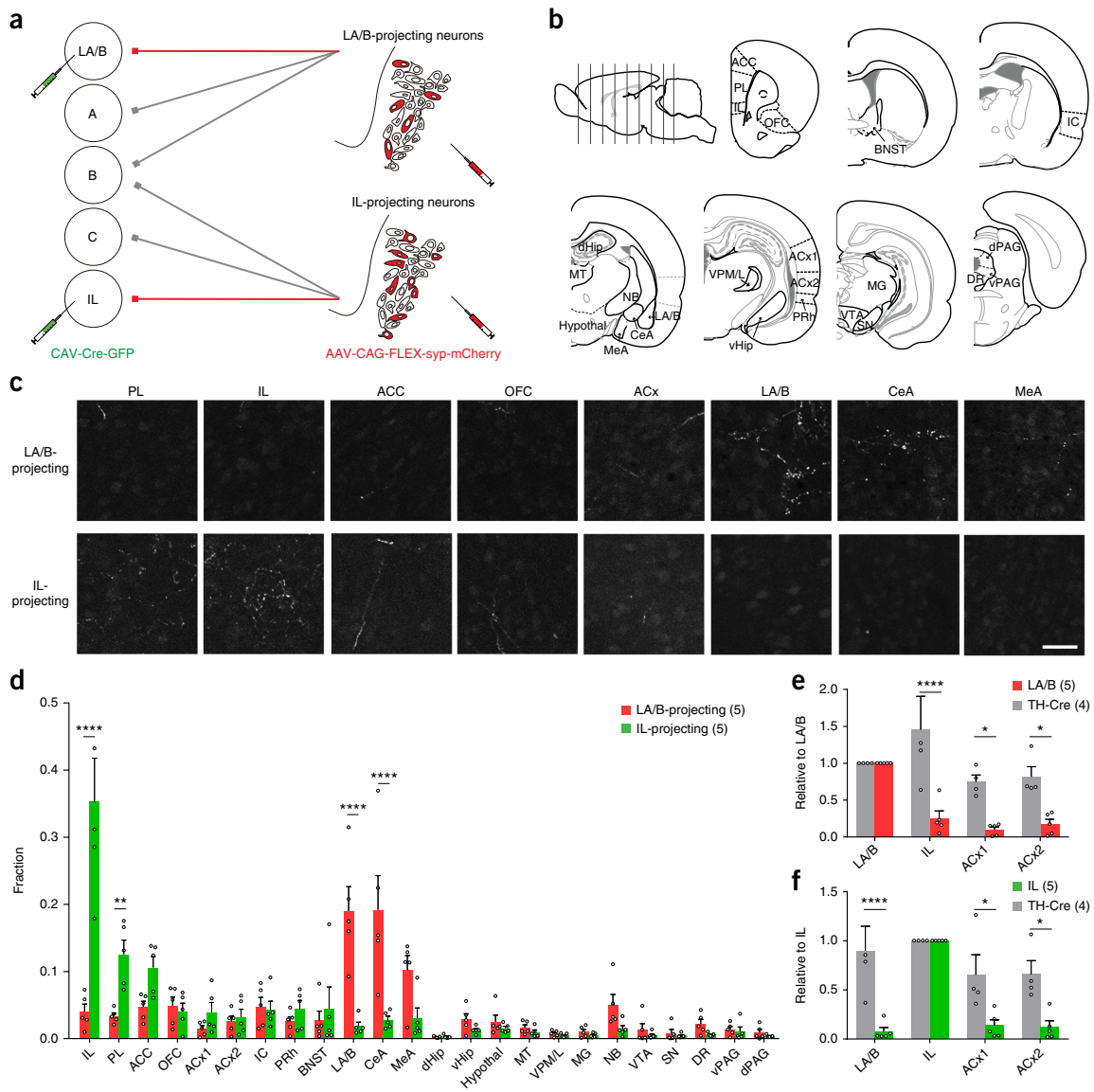
To probe the functional role of these anatomically distinct LC noradrenaline subpopulations in fear and extinction learning, we performed a series of optogenetic studies using recombinant rabies viral vectors carrying a construct encoding a light-activated inhibitory archaerhodopsin + enhanced GFP fusion protein (RVΔG-eArchT3.0-EGFP; Fig. 3g–i)^{27,35}. This virus is taken up by synaptic terminals and transported retrogradely to cell bodies that project to the injected region. Using this approach (Fig. 3h,i and Supplementary Fig. 7a,b), we optogenetically inhibited the activity of amygdala- or mPFC-projecting LC noradrenaline neurons in isolation. Inactivation of LA/B-projecting noradrenaline neurons during the aversive shock period of fear conditioning significantly reduced fear memory formation (Fig. 3h,j), whereas inactivation of IL-projecting neurons had no effect (Fig. 3i,k). By contrast, inactivation of IL-projecting neurons during the auditory CS period of fear extinction impaired acquisition of extinction learning, as these animals exhibited sustained auditory-evoked freezing responses during and 24 h after extinction training (Fig. 3m). Unexpectedly, inactivation of LA/B-projecting LC noradrenaline neurons during the auditory CS period of extinction enhanced consolidation of extinction memories, as freezing was lower 24 h after extinc-

tion learning (Fig. 3l). Inactivation of either of these cell populations during the auditory CS period 24 h after extinction learning had occurred had no effect on freezing responses, demonstrating that these cell populations are not involved in recalling extinction memories (Supplementary Fig. 8a,b).

We next tested whether optogenetic activation of these different cell populations affected fear or extinction learning and memory by injecting retrogradely transported canine adenoviral vectors carrying a construct encoding Cre-recombinase (CAV-Cre) into the IL or LA followed by injections of AAV vectors carrying a construct encoding a Cre-dependent channelrhodopsin + monomeric Azami-Green fusion protein (AAV-ChR2-mAG1) into the LC (Fig. 4a,b). Optogenetic stimulation of LA/B-projecting neurons during the shock US period of weak fear conditioning enhanced learning (Fig. 4c), while stimulating IL-projecting cells had no effect (Fig. 4d). Pairing auditory CS with optical stimulation of LA/B-projecting cells alone as a US was not sufficient to produce fear conditioning (ChR2: $4.14\% \pm 0.53\%$ freezing; mAG1: $7.70\% \pm 2.00\%$ freezing; $t_4 = 1.718$, $P = 0.1367$). By contrast, stimulating LA/B-projecting cells during the tone period of fear extinction had no effect on learning (Fig. 4e). However, optogenetic stimulation of IL-projecting cells reduced the consolidation of extinction learning (Fig. 4f). Notably, this attenuation of extinction consolidation through overstimulation of IL-projecting cells was blocked if an alpha-1 adrenergic receptor antagonist (Prazosin) was microinjected into the IL before extinction training (Fig. 4g,i). On its own, the drug did not affect fear expression or within-session extinction, but it did reduce

long-term retention of extinction, similarly to the findings of a previous report³⁶ (Fig. 4h,j). Together, this suggests that high levels of noradrenaline release enhances fear learning (through

engagement of amygdala projecting LC neurons) and dysregulates extinction through recruitment of mPFC-projecting LC neurons and α -1-ARs in mPFC.



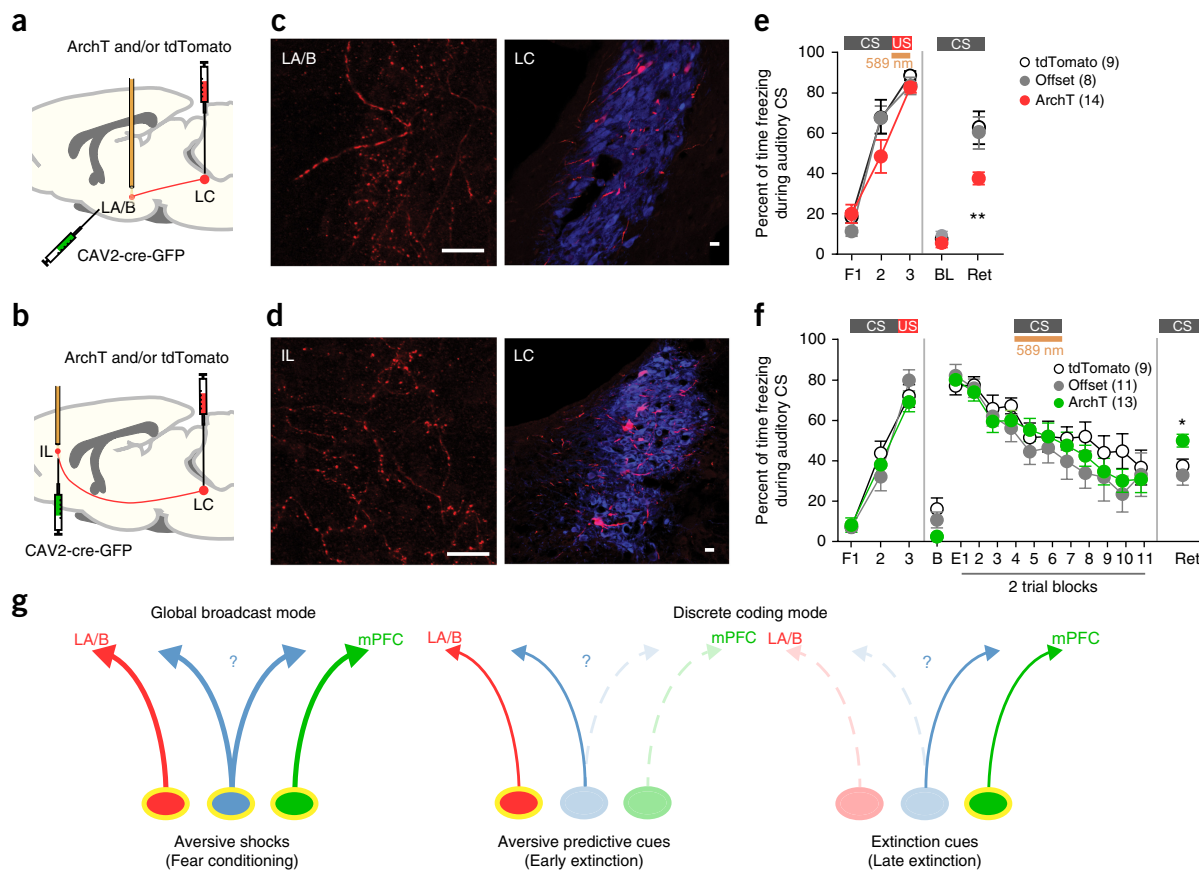


Figure 6 Specific axon terminal fields from defined LC noradrenaline cell populations contribute to fear or extinction memory formation. **(a,b)** Schematic of CAV2-Cre-GFP injection into LA/B or IL combined with AAV-ArchT-tdTomato or AAV-tdTomato into LC. **(c,d)** Example images of ArchT-tdTomato expression in LC cell bodies (right) and nerve terminals (left) from amygdala-projecting **(c)** or IL-projecting **(d)** cells. Scale bars, 20 μ m. **(e)** Inhibition of axon terminals in LA/B during the shock-US reduced memory formation, as freezing was significantly attenuated during the retrieval test (right; $F_{2,28} = 7.57$, $P = 0.0024$, one-way ANOVA). **(f)** Inhibition of axon terminals in IL during the auditory CS period of extinction had no effect during the extinction session (interaction, $F_{20,260} = 0.64$, $P = 0.88$; main effect of group, $F_{2,26} = 0.72$, $P = 0.49$, two-way RM ANOVA) but reduced the consolidation of extinction memories, as freezing responses significantly increased and/or recovered during the extinction retrieval test in the ArchT group compared with controls ($F_{2,26} = 5.95$, $P = 0.0074$, one-way ANOVA). Data represent the mean \pm s.e.m.; numbers in parentheses represent the number of samples. For all graphs: Newman-Keuls *post hoc* tests, * $P < 0.05$, ** $P < 0.01$. **(g)** Hypothetical interpretative model of LC function. Yellow lines around cell bodies indicate activated cells and line width and arrowhead size denotes strength of activation. Left: strong shock-evoked activation of large populations of LC noradrenaline neurons during fear conditioning (including other unknown populations (blue, "?"). Middle: moderate activation of discrete populations of LC noradrenaline cells during early extinction, when auditory cues predict aversive outcomes. Right: moderate activation of different cell populations of later in extinction.

Efferent mapping of functionally distinct LC noradrenaline cell populations

Contrary to the traditional idea that LC noradrenaline neurons collateralize broadly and innervate many brain regions, our data demonstrate anatomical and functional specificity of certain populations of noradrenaline neurons based on their innervation of amygdala or mPFC. However, with the dual tracer injection approach we used above, it was unclear whether these amygdala- and mPFC-projecting LC noradrenaline cell populations were specifically connected with individual targets or whether they also collateralized broadly and innervated many other brain regions. Using modern viral tracing techniques that allow for brain-wide mapping of efferent projections⁸, we next examined the degree of specificity and/or overlap and the breadth these functionally distinct cell populations exhibit in their efferent connectivity. To do this, we injected retrograde canine adenoviral vectors carrying a construct encoding Cre-recombinase fused to GFP (CAV2-Cre-GFP)³⁷ into either the IL or LA/B, followed by injections of AAV vectors carrying a construct encoding a

Cre-dependent synaptophysin (a synaptic vesicle protein enriched at neurotransmitter release sites) fused to mCherry into the LC (**Fig. 5a**). This resulted in the expression of mCherry in the brain-wide axonal arbors of each noradrenaline cell population. Using this approach, we quantified the axonal projection patterns of each cell population throughout the brain (**Fig. 5b**). We found that amygdala-projecting LC cells innervated both LA/B and the central nucleus of the amygdala significantly more strongly than mPFC-projecting LC neurons (**Fig. 5c,d** and **Supplementary Fig. 9a**). By contrast, IL-projecting neurons innervated the IL and the prelimbic subregion of the mPFC significantly more than amygdala-projecting LC neurons (**Fig. 5d**). While both cell populations innervated many other areas throughout the brain, the innervation of other brain regions outside of amygdala or mPFC appeared very weak.

To better approximate the strength of innervation of these projection-defined LC noradrenaline neurons relative to an approximation of the total LC noradrenaline innervation, we injected AAV-synaptophysin-mCherry into the LC of TH-Cre rats and analyzed the efferent

innervation patterns of general, non-projection-defined LC neurons (Supplementary Fig. 9b,c). We calculated the TH-Cre innervation of IL and LA/B and compared this with the density of innervation from the IL- or LA/B-projecting LC neurons using the CAV2-Cre approach described above. We also compared this with the innervation of the auditory cortex (regions 1 and 2) by LC TH⁺ cells as well as by IL- and LA/B-projecting LC cells. We analyzed auditory cortex as a representative brain region for comparison of innervation because it was equally innervated by both mPFC- and LA/B-projecting cell populations (Fig. 5d and Supplementary Fig. 9a) and because another study has shown that it is innervated by a population of broadly connected LC noradrenaline neurons⁸. We found that the density of terminal innervations of IL or LA/B were similar between CAV2-Cre-injected (in IL or LA/B, respectively) and TH-Cre-injected animals (Supplementary Fig. 9b–c), providing validation of the approach. However, the axonal density in a given target region relative to the TH-Cre innervation and to the innervation of each cell population based on where the CAV2-Cre was injected was much lower in the auditory cortex from both LA/B- and IL-projecting cells (Fig. 5e,f and Supplementary Fig. 9b,c). Together, these data suggest that despite their strong innervation of IL or LA/B, these different LC noradrenaline neuronal subpopulations are only weakly connected with other brain regions. In contrast to traditional views of LC function, this directly supports the idea that some LC noradrenaline neurons are specifically connected with their target structures and exhibit more minor collateralization to other brain regions.

Efferent projections target specific control of fear and extinction learning

To address whether LC innervation of amygdala or mPFC was functionally important for fear and extinction learning, we next asked whether inhibition of the nerve terminals of these different LC noradrenaline neuronal populations in these regions affected fear or extinction learning. To test this question, we injected CAV2-Cre-GFP into the LA/B or mPFC and injected AAV vectors carrying a construct encoding Cre-dependent ArchT-tdTomato into the LC (Fig. 6a,b). This produced expression of ArchT-tdTomato in the cell bodies and nerve terminals of these different noradrenaline cell populations (Fig. 6c,d), making it possible to optically inhibit the terminals of these cells in the amygdala or mPFC. Because we saw large effects of manipulating amygdala-projecting cells on fear learning and mPFC-projecting cells on extinction, we restricted our terminal manipulation experiments to these cell populations and behaviors. Using this approach, we first optically inactivated the noradrenaline terminals of the amygdala-projecting LC cells in the LA/B during the shock period of fear learning. We used ArchT in these experiments because it expresses optimally in nerve terminals and has been shown to inhibit neurotransmitter release, particularly with short-duration illumination protocols in which paradoxical neurotransmitter release is not evident^{38,39}. Like cell-body inhibition, this terminal-specific manipulation of LA/B-projecting cells reduced fear learning (Fig. 6e). By contrast, terminal inhibition of mPFC-projecting LC noradrenaline cell populations in the IL reduced extinction memory consolidation (Fig. 6f). However, unlike the effects of the cell-body manipulations (Fig. 3m), this manipulation did not affect the initial learning of extinction, consistent with the idea that the IL is important in storing and/or consolidating extinction memories. This suggests that projections to other target sites and/or local interactions between LC subpopulations of cells also participated in this process. Together, these findings show that, in addition to specific anatomical connectivity, activity in the terminal fields of these cells in the

amygdala or mPFC contributes functionally to producing behavioral fear and extinction learning.

DISCUSSION

Here we demonstrate a modular organization in the LC noradrenaline system in which differential response modes are multiplexed across distinct cell populations with specific efferent connectivity to dynamically control opposing adaptive learning states (Fig. 6g). Firing-rate responses of LC neurons were heterogeneous and patterned, with different populations of cells responding discretely and moderately to aversive or safety predictive cues following fear or extinction learning. However, the same populations were robustly co-activated in response to more intense aversive experiences such as shock USs, exhibiting a stronger, unified noradrenaline signal. The ability of LC neurons to switch between a global broadcast mode versus a discrete, patterned coding mode allows the LC to flexibly mediate general arousal and emotional learning functions in parallel with more precise control in response to ambiguous and dynamic adaptive requirements. These differences in response properties can be explained by a learning-dependent shift in the balance of predictive cue-evoked activity in anatomically defined cell populations, with higher levels of activation in amygdala-projecting cells during fear states and higher levels of activity in mPFC-projecting neurons during extinction learning states. Notably, under normal learning conditions these cell modules are differentially involved in fear and extinction learning and exhibit specific connectivity with amygdala or mPFC. However, stronger artificial activation of amygdala-projecting LC cells facilitated weak fear learning, while overstimulation of mPFC-projecting LC cells disrupted the retention of extinction memories through activation of α -1-ARs in mPFC. Together, these functional and anatomical features of LC, combined with state-dependent response properties, enable precise spatial control and amplitude control of noradrenaline release. These results provide a unified framework explaining how this important neuromodulatory system regulates diverse adaptive functions, in this case the balance between emotional fear learning and extinction of fear responses when they are no longer appropriate.

One notable aspect of our findings is that indiscriminate inhibition of many LC noradrenaline cells had less of an effect on fear conditioning and/or extinction than did more-targeted inhibition of amygdala- or mPFC-projecting cell populations. While the reasons for this are not entirely clear, one possibility supported by the data is that global inhibition of LC neurons may affect functionally opposing cell populations, resulting in more modest behavioral effects, while more-targeted inhibition of specific cell populations produces more robust behavioral consequences. In fact, other studies have seen this type of dissociation when manipulating global versus specific projection-defined populations of mPFC neurons⁴⁰. Further supporting this idea, studies have found mixed results of global LC manipulations on fear conditioning, while brain-region-specific pharmacological interventions have revealed clearer effects on behavior^{19,29,41}. Finally, it is not clear whether the individual amygdala- and mPFC-projecting cell populations contribute uniquely to aversive learning and/or extinction or more generally to other forms of emotional or flexible learning. One paper reports that β -AR activity in mPFC is necessary for appetitive extinction learning⁴², suggesting a more general function for mPFC-projecting LC neurons. By contrast, a recently published paper demonstrated that optogenetic stimulation of LC inputs to the LA/B enhances anxiety and produces place aversion, suggesting that this projection is more specific for aversive learning and behavior¹⁸.

These findings help to clarify opposing views of this neuromodulatory system. Past work has suggested both homogeneity^{8–12} and heterogeneity^{6,8,10,13–17} in LC organization, based on anatomical, morphological, physiological or molecular characteristics. However, no study has examined LC organization from a functional behavioral perspective alongside anatomical and physiological considerations. Using this comprehensive approach, our results argue against the simple interpretation of the LC as a purely homogeneous, highly colateralized population of cells and instead suggest a modular organization of noradrenaline neurons in this region. Furthermore, we show that LC neurons can be engaged strongly or weakly and homogeneously as an ensemble or heterogeneously depending on task demands. This feature could underlie the ability of the LC to provide a global brain-arousal signal on some occasions, while at other times regulating specific and even opposing brain functions. Our data do not rule out the possibility that other populations of LC cells are broadly projecting, an idea supported by recent anatomical work⁸. In addition, molecular, morphological and topographic features of the LC may also delineate certain LC modules⁶. Although we did not observe task-dependent changes in spontaneous tonic firing rates that other studies have reported using different behavioral paradigms⁷, it is likely that under different task conditions tonic changes may provide another coding scheme in LC neurons. Building on this new framework, it will be important in future studies to further examine the logic of this modular organization, how local connectivity and long-range afferent inputs control LC neural activity and module coordination with context dependence, how different types of signals influence downstream structures, and how these findings relate to important theories of LC function^{1,5,7,43}.

Our results also reveal how the balance between fear and extinction learning arises through modular organization, the dual response modes of LC neurons and different adrenergic receptor sensitivities in downstream projection targets. One theory of LC noradrenaline neuron function suggests that the balance between emotional learning and cognitive-behavioral flexibility is controlled through global adjustments in the level of noradrenaline release. According to this idea, high noradrenaline levels evoked by stress engage the amygdala to enhance emotional, reflexive behaviors and at the same time deactivate mPFC through recruitment of α -1-ARs to reduce cognitive flexibility⁵. Our results are consistent with this model but suggest that this differential regulation arises through a modularly organized LC circuit. Specifically, we found that most LC neurons were activated strongly by aversive shocks and that inhibition of shock responding in amygdala projecting LC neurons or their terminals in the LA/B reduced fear learning. Furthermore, optogenetically overstimulating amygdala-projecting cells enhanced weak fear conditioning, consistent with prior results using pharmacological stimulation of β -ARs in LA⁴⁴. Although we saw no effect of manipulating mPFC-projecting cells during fear learning, it is possible that their strong shock-evoked activation disengages mPFC networks and reduces the switch to more flexible behavioral states^{4,5,45}. Supporting this idea, we found that overstimulating mPFC-projecting LC noradrenaline cells during extinction reduced the persistence of extinction memories, an effect that was dependent on activation of mPFC α -1-ARs, a relatively less noradrenaline-sensitive AR subtype. During extinction learning, we found that LC neurons switched to a more discrete activation mode, in which one population of LC neurons was moderately activated by fear-inducing cues during early extinction and another population began responding in late extinction periods. Our activity-dependent imaging results suggest that this reflects a switch in the balance of activity from LA/B- to mPFC-projecting cell populations. Together

with the behavioral findings demonstrating functional competition of these cell populations during extinction learning, this indicates that the balance of activity across these two cell populations during extinction is critical for the switch from fear responding to behavioral flexibility. The finding that both inhibiting and enhancing auditory CS-evoked responding beyond normal levels in the mPFC-projecting cells reduced extinction learning and memory suggests an inverted-U function for the effects of noradrenaline on behavioral flexibility, arising specifically from this noradrenaline cell population.

One important question arising from these results concerns the mechanisms within the amygdala and mPFC through which noradrenaline exerts its effects on behavior. Neuronal plasticity in the lateral amygdala (LA), mediating fear learning, is dependent on parallel β -AR-dependent and Hebbian-mediated processes²⁰, although the detailed local circuit and molecular mechanisms whereby noradrenaline modulates learning are not clear. One possibility is that, within LA pyramidal neurons, β -AR activity through cAMP signaling cascades synergizes with faster, calcium-mediated signaling induced by Hebbian plasticity to strengthen short- and long-term memory induction and consolidation mechanisms^{20,44}. Another possibility is that noradrenaline reduces local feedforward and feedback GABAergic activity⁴⁶ and/or modulates LA pyramidal cell excitability⁴⁷, thereby facilitating Hebbian plasticity mechanisms. Regarding the projections to the mPFC, it is less clear how noradrenaline acting on mPFC β -ARs and α -1-ARs (as we report here) modulates extinction learning. One possibility is that, in conjunction with NMDA receptor activation, noradrenaline increases the excitability of pyramidal neurons through β -AR activation to modulate the consolidation of extinction learning^{25,48}. It will be important in future studies to address these questions using cell-type-specific molecular biological approaches.

The discovery of LC functional modularity for fear and extinction learning is particularly relevant to stress-related psychiatric disorders, such as anxiety. Prolonged and/or intense stress and trauma can produce anxiety disorders with exaggerated aversive learning and persistent fear memories. The LC noradrenaline system is prominently dysregulated by stress^{1–4,45}, and identifying how stress affects the balance of activity across different LC noradrenaline cell modules will be essential for understanding the etiology of stress-induced anxiety disorders. Moreover, the LC noradrenaline system is a promising drug target for the treatment of psychiatric anxiety disorders^{4,49,50}. Given the heterogeneity in LC noradrenaline cell populations we report related specifically to clinical features of post-traumatic stress disorder, more refined drug targeting of these fear-learning versus extinction-promoting cell populations could substantially improve the efficacy of noradrenaline-based treatment approaches.

METHODS

Methods, including statements of data availability and any associated accession codes and references, are available in the [online version of the paper](#).

Note: Any Supplementary Information and Source Data files are available in the online version of the paper.

ACKNOWLEDGMENTS

We thank M. Iwasaki, A. Umetsu, K. Mori and A. Krejcirikova for excellent technical assistance and H. Hamanaka for setting up rabies virus production in the lab. We thank C. Yokoyama, A. Luthi, H. Schiff, T. Shimogori, S. Fujisawa, T. McHugh, A. Benucci and members of the Johansen lab for comments on earlier versions of the manuscript. We also thank J. Kleinschmidt (German Cancer Research Center) for his gift of the AAV helper vectors and the RIKEN Research Resources Center for help with viral titration. This work was supported by RIKEN SPRP (A.U. and B.Z.T.), KAKENHI 16H01291, 15H04264, 15H01301 (J.P.J.),

16K21620 (B.Z.T.), 26750380, 16H05928 (A.U.)) and the Strategic Research Program for Brain Sciences from the Ministry of Education, Culture, Sports, Science and Technology (11041047, J.P.J.).

AUTHOR CONTRIBUTIONS

A.U., B.Z.T. and J.P.J. designed the experiments and wrote up the manuscript. A.U., B.Z.T., E.A.Y., J.S.C. and J.K. carried out the experiments. A.U., B.Z.T. and J.P.J. analyzed the results. F.J. and E.J.K. supplied viral reagents before publication and expert advice on their use. I.B.W. and K.D. supplied viral reagents and transgenic animals before publication as well as expert advice on their use.

COMPETING FINANCIAL INTERESTS

The authors declare no competing financial interests.

Reprints and permissions information is available online at <http://www.nature.com/reprints/index.html>. Publisher's note: Springer Nature remains neutral with regard to jurisdictional claims in published maps and institutional affiliations.

- Sara, S.J. & Bouret, S. Orienting and reorienting: the locus coeruleus mediates cognition through arousal. *Neuron* **76**, 130–141 (2012).
- McCall, J.G. *et al.* CRH engagement of the locus coeruleus noradrenergic system mediates stress-induced anxiety. *Neuron* **87**, 605–620 (2015).
- Valentino, R.J. & Van Bockstaele, E. Convergent regulation of locus coeruleus activity as an adaptive response to stress. *Eur. J. Pharmacol.* **583**, 194–203 (2008).
- Maren, S. & Holmes, A. Stress and fear extinction. *Neuropsychopharmacology* **41**, 58–79 (2016).
- Arnsten, A.F. Stress signalling pathways that impair prefrontal cortex structure and function. *Nat. Rev. Neurosci.* **10**, 410–422 (2009).
- Berridge, C.W. & Waterhouse, B.D. The locus coeruleus-noradrenergic system: modulation of behavioral state and state-dependent cognitive processes. *Brain Res. Brain Res. Rev.* **42**, 33–84 (2003).
- Aston-Jones, G. & Cohen, J.D. An integrative theory of locus coeruleus-norepinephrine function: adaptive gain and optimal performance. *Annu. Rev. Neurosci.* **28**, 403–450 (2005).
- Schwarz, L.A. *et al.* Viral-genetic tracing of the input-output organization of a central noradrenergic circuit. *Nature* **524**, 88–92 (2015).
- Nakamura, S. & Iwama, K. Antidromic activation of the rat locus coeruleus neurons from hippocampus, cerebral and cerebellar cortices. *Brain Res.* **99**, 372–376 (1975).
- Nagai, T., Satoh, K., Imamoto, K. & Maeda, T. Divergent projections of catecholamine neurons of the locus coeruleus as revealed by fluorescent retrograde double labeling technique. *Neurosci. Lett.* **23**, 117–123 (1981).
- Room, P., Postema, F. & Korf, J. Divergent axon collaterals of rat locus coeruleus neurons: demonstration by a fluorescent double labeling technique. *Brain Res.* **221**, 219–230 (1981).
- Foote, S.L., Bloom, F.E. & Aston-Jones, G. Nucleus locus ceruleus: new evidence of anatomical and physiological specificity. *Physiol. Rev.* **63**, 844–914 (1983).
- Chandler, D.J., Gao, W.J. & Waterhouse, B.D. Heterogeneous organization of the locus coeruleus projections to prefrontal and motor cortices. *Proc. Natl. Acad. Sci. USA* **111**, 6816–6821 (2014).
- Li, Y. *et al.* Retrograde optogenetic characterization of the pontospinal module of the locus coeruleus with a canine adenoviral vector. *Brain Res.* **1641**, 274–290 (2016).
- Bouret, S. & Richmond, B.J. Relation of locus coeruleus neurons in monkeys to Pavlovian and operant behaviors. *J. Neurophysiol.* **101**, 898–911 (2009).
- Kalwani, R.M., Joshi, S. & Gold, J.I. Phasic activation of individual neurons in the locus coeruleus/subcoeruleus complex of monkeys reflects rewarded decisions to go but not stop. *J. Neurosci.* **34**, 13656–13669 (2014).
- Kebschull, J.M. *et al.* High-throughput mapping of single-neuron projections by sequencing of barcoded RNA. *Neuron* **91**, 975–987 (2016).
- McCall, J.G. *et al.* Locus coeruleus to basolateral amygdala noradrenergic projections promote anxiety-like behavior. *eLife* **6**, e18247 (2017).
- Bush, D.E., Caparosa, E.M., Gekker, A. & Ledoux, J. Beta-adrenergic receptors in the lateral nucleus of the amygdala contribute to the acquisition but not the consolidation of auditory fear conditioning. *Front. Behav. Neurosci.* **4**, 154 (2010).
- Johansen, J.P. *et al.* Hebbian and neuromodulatory mechanisms interact to trigger associative memory formation. *Proc. Natl. Acad. Sci. USA* **111**, E5584–E5592 (2014).
- LeDoux, J.E. Coming to terms with fear. *Proc. Natl. Acad. Sci. USA* **111**, 2871–2878 (2014).
- Herry, C. & Johansen, J.P. Encoding of fear learning and memory in distributed neuronal circuits. *Nat. Neurosci.* **17**, 1644–1654 (2014).
- LeDoux, J.E. Emotion circuits in the brain. *Annu. Rev. Neurosci.* **23**, 155–184 (2000).
- Quirarte, G.L., Galvez, R., Roozendaal, B. & McGaugh, J.L. Norepinephrine release in the amygdala in response to footshock and opioid peptidergic drugs. *Brain Res.* **808**, 134–140 (1998).
- Mueller, D., Porter, J.T. & Quirk, G.J. Noradrenergic signaling in infralimbic cortex increases cell excitability and strengthens memory for fear extinction. *J. Neurosci.* **28**, 369–375 (2008).
- Hugues, S., Garcia, R. & Léna, I. Time course of extracellular catecholamine and glutamate levels in the rat medial prefrontal cortex during and after extinction of conditioned fear. *Synapse* **61**, 933–937 (2007).
- Han, X. *et al.* A high-light sensitivity optical neural silencer: development and application to optogenetic control of non-human primate cortex. *Front. Syst. Neurosci.* **5**, 18 (2011).
- Witten, I.B. *et al.* Recombinase-driver rat lines: tools, techniques, and optogenetic application to dopamine-mediated reinforcement. *Neuron* **72**, 721–733 (2011).
- Murchison, C.F. *et al.* A distinct role for norepinephrine in memory retrieval. *Cell* **117**, 131–143 (2004).
- McGaugh, J.L. The amygdala modulates the consolidation of memories of emotionally arousing experiences. *Annu. Rev. Neurosci.* **27**, 1–28 (2004).
- Martins, A.R. & Froemke, R.C. Coordinated forms of noradrenergic plasticity in the locus coeruleus and primary auditory cortex. *Nat. Neurosci.* **18**, 1483–1492 (2015).
- Rasmussen, K. & Jacobs, B.L. Single unit activity of locus coeruleus neurons in the freely moving cat. II. Conditioning and pharmacologic studies. *Brain Res.* **371**, 335–344 (1986).
- Sara, S.J. & Segal, M. Plasticity of sensory responses of locus coeruleus neurons in the behaving rat: implications for cognition. *Prog. Brain Res.* **88**, 571–585 (1991).
- Swanson, L.W. The locus coeruleus: a cytoarchitectonic, Golgi and immunohistochemical study in the albino rat. *Brain Res.* **110**, 39–56 (1976).
- Mattis, J. *et al.* Principles for applying optogenetic tools derived from direct comparative analysis of microbial opsins. *Nat. Methods* **9**, 159–172 (2011).
- Do-Monte, F.H., Alenxworth, M. & Carobrez, A.P. Impairment of contextual conditioned fear extinction after microinjection of alpha-1-adrenergic blocker Prazosin into the medial prefrontal cortex. *Behav. Brain Res.* **211**, 89–95 (2010).
- Soudais, C., Laplace-Builhe, C., Kissa, K. & Kremer, E.J. Preferential transduction of neurons by canine adenovirus vectors and their efficient retrograde transport *in vivo*. *FASEB J.* **15**, 2283–2285 (2001).
- Mahn, M., Prigge, M., Ron, S., Levy, R. & Yizhar, O. Biophysical constraints of optogenetic inhibition at presynaptic terminals. *Nat. Neurosci.* **19**, 554–556 (2016).
- Ozawa, T. *et al.* A feedback neural circuit for calibrating aversive memory strength. *Nat. Neurosci.* **20**, 90–97 (2017).
- Warden, M.R. *et al.* A prefrontal cortex-brainstem neuronal projection that controls response to behavioural challenge. *Nature* **492**, 428–432 (2012).
- Uematsu, A., Tan, B.Z. & Johansen, J.P. Projection specificity in heterogeneous locus coeruleus cell populations: implications for learning and memory. *Learn. Mem.* **22**, 444–451 (2015).
- Latagliata, E.C., Saccoccio, P., Milia, C. & Puglisi-Allegra, S. Norepinephrine in prefrontal cortex delays extinction of amphetamine-induced conditioned place preference. *Psychopharmacology (Berl.)* **233**, 973–982 (2016).
- Yu, A.J. & Dayan, P. Uncertainty, neuromodulation, and attention. *Neuron* **46**, 681–692 (2005).
- Schiff, H.C. *et al.* β -Adrenergic receptors regulate the acquisition and consolidation phases of aversive memory formation through distinct, temporally regulated signaling pathways. *Neuropsychopharmacology* **42**, 895–903 (2017).
- Fitzgerald, P.J., Giustino, T.F., Seemann, J.R. & Maren, S. Noradrenergic blockade stabilizes prefrontal activity and enables fear extinction under stress. *Proc. Natl. Acad. Sci. USA* **112**, E3729–E3737 (2015).
- Tully, K., Li, Y., Tsvetkov, E. & Bolshakov, V.Y. Norepinephrine enables the induction of associative long-term potentiation at thalamo-amygdala synapses. *Proc. Natl. Acad. Sci. USA* **104**, 14146–14150 (2007).
- Faber, E.S. *et al.* Modulation of SK channel trafficking by beta adrenoceptors enhances excitatory synaptic transmission and plasticity in the amygdala. *J. Neurosci.* **28**, 10803–10813 (2008).
- Burgos-Robles, A., Vidal-Gonzalez, I., Santini, E. & Quirk, G.J. Consolidation of fear extinction requires NMDA receptor-dependent bursting in the ventromedial prefrontal cortex. *Neuron* **53**, 871–880 (2007).
- Giustino, T.F., Fitzgerald, P.J. & Maren, S. Revisiting propranolol and PTSD: memory erasure or extinction enhancement? *Neurobiol. Learn. Mem.* **130**, 26–33 (2016).
- Belkin, M.R. & Schwartz, T.L. Alpha-2 receptor agonists for the treatment of posttraumatic stress disorder. *Drugs Context* **4**, 212286 (2015).

ONLINE METHODS

Animals. All experimental procedures were approved by the Animal Care and Use Committees of the RIKEN Brain Science Institute. Male adult Long-Evans or TH-Cre rats (8–12 weeks old at the time of surgery) were used for all experiments except for the retrograde tracing study (**Supplementary Fig. 5g**), which was done in male C57/BL mice (9 weeks old at the time of surgery). The vivarium was maintained at constant temperature (23 ± 1 °C) with a 12:12 light:dark cycle (lights on 7 a.m. to 7 p.m.). Animals were singly housed and food and water were provided *ad libitum*. The TH-Cre breeding colony was maintained by mating wild-type female rats with TH-Cre male rats. All behavioral and electrophysiological experiments were done between 9 a.m. and 6 p.m.

Viruses. Adeno-associated virus (serotype 9)-CAG promoter-flip excision-archaerhodopsin T-GFP (AAV9-CAG-FLEX-ArchT-GFP), AAV9-CAG-FLEX-GFP, AAV9-CAG-FLEX-ArchT-tdTomato and AAV9-CAG-FLEX-tdTomato were obtained from the University of North Carolina VectorCore. Canine adenovirus (CAV2)-Cre-GFP and CAV2-Cre were generated by the Kremer lab and given to the Montpellier vector core for distribution prior to publication. AAV9-CAG-FLEX-ChR2-mAG1 (monomeric Azami-Green-1), AAV9-CAG-FLEX-mAG1, AAV9-CAG-FLEX-synaptophysin-mCherry, Rabies virus (RVΔG)-eArchT3.0-EGFP^{35,51} and RVΔG-EGFP were produced and packaged in our lab. We thank K. Conzelmann (Ludwig-Maximilians-University Munich) for the generous gift of the N, P, L and G pTIT-expressing plasmids^{52,53} and I. Wickersham (Massachusetts Institute of Technology) and J.A.T. Young (Salk Institute) for the generous gift of the BHK-B19G2 cell line used for rabies virus production.

Surgery. All surgeries were performed under aseptic conditions with isoflurane anesthesia (3–5% for induction, 1.5–3% for maintenance). For electrophysiology, rats were secured in a stereotaxic frame, injected with AAV9-FLEX-ArchT-GFP and implanted with a drivable optrode (a custom-built array of 8 tetrodes or 16 stereotrodes glued to 200- μ m optic fibers) in the unilateral LC (AP: -1.2 mm from interaural line, which corresponded to variable distances from bregma (AP: -9.6 to -10.2 mm, ML: ± 4.5 mm, DV: -5.1 mm, 30° angle). To deliver periorbital shock stimulus, rats were also implanted with a pair of insulated stainless steel wires beneath the skin of the contralateral eyelid. For ArchT behavioral experiments, rats received bilateral virus injections and fiber implantations above the LC at the following coordinates; LC (AP: -9.6 to -10.2 mm, ML: ± 4.55 mm, DV: -5.5 mm for 1 μ l of AAV; and ML: ± 4.55 mm, DV: -5.5 mm for fiber, 30° angle), LA/B (AP: -2.1 and -3.1 mm, ML: ± 5.2 mm, DV: -8.8 mm; 0.4 μ l of RVΔG at each site) and IL (AP: +3.0 and +2.6 mm, ML: ± 2.9 mm, DV: -4.2 mm, 30° angle; 0.4 μ l of RVΔG at each site). For ChR2 experiments, 0.4 μ l of CAV2-Cre was bilaterally injected into either LA/B (AP: -2.6, ML: ± 5.2 mm, DV: -8.8 mm) or IL (AP: +2.7 mm, ML: ± 2.9 mm, DV: -4.2 mm, 30° angle), and 1 μ l of AAV-FLEX-ChR2-mAG1/mAG1 was bilaterally injected into the LC at the abovementioned coordinates. For ChR2 stimulation combined with pharmacology experiments, CAV2-Cre was bilaterally injected into IL, AAV-FLEX-ChR2-mAG1 was bilaterally injected into the LC at the abovementioned coordinates and bilateral guide cannulae were implanted above IL (AP: +2.7 mm, ML: ± 2.9 mm, DV: -2.8 mm, 30° angle), along with optical fibers in LC. For the terminal-inhibition behavioral study, rats received bilateral CAV2-Cre-GFP injections and fiber implantation above either LA/B (AP: -3.2 mm, ML: ± 5.4 mm, DV: -8.6 mm for 0.3 μ l of CAV2 and -7.6 mm for fiber) or IL (AP: +2.7 mm, ML: ± 2.9 mm, DV: -4.2 mm for 0.3 μ l of CAV2 and -3.7 mm for fiber; 30° angle), and AAV-FLEX-ArchT-tdTomato/tTomato was injected into the bilateral LC at the abovementioned coordinates. All implants were secured using Super-Bond cement (SunMedical) and acrylic dental cement. Behavioral experiments began after 3–7 d (for rabies experiments, all experiments were finished within 8 d), 3 weeks (for TH-Cre and ChR2 experiments) or 6 weeks (terminal inhibition experiments) of incubation time. For retrograde tracing study, 0.3 μ l of each tracer (green and red Retrobeads, Lumafluor Inc.; cholera toxin subunit B Alexa Fluor 647-conjugate, Thermo Fisher Scientific Inc.) were injected into ipsilateral LA/B (AP: -2.6 mm, ML: +5.2 mm, DV: -8.8 mm) and IL (AP: +2.8 mm, ML: +2.9 mm, DV: -4.2 mm, 30° angle). Rats were subjected to behavioral experiments (for the c-Fos experiment) and/or killed for analysis 1 week after surgery. For the retrograde tracing study in mice, 0.3 μ l of each tracer (green and red Retrobeads, Lumafluor Inc.) were injected into ipsilateral LA/B (AP: -1.7 mm, ML: +3.4 mm, DV: -4.3 mm) and IL

(AP: +1.8 mm, ML: +1.8 mm, DV: -2.5 mm, 30° angle). Mice were killed for analysis 1 week after surgery. For the efferent mapping study, 0.4 μ l of CAV2-Cre-GFP was injected into either LA/B (AP: -2.6 mm, ML: ± 5.2 mm, DV: -8.8 mm) or IL (AP: +2.7 mm, ML: ± 2.9 mm, DV: -4.2 mm, 30° angle) unilaterally, and 1 μ l of AAV-FLEX-synaptophysin-mCherry was injected into the ipsilateral LC at the abovementioned coordinates. The central nucleus of the amygdala (CeA) does not send projections to the LA/B. Based on this knowledge, we adjusted the injection volume of CAV2-Cre-GFP to avoid GFP expression in CeA and used this to estimate optimal injection volume and CAV2 viral spread. Rats were killed for analysis 6 weeks after surgery.

Fear conditioning and extinction. Animals were randomly assigned to experimental groups before the start of each experiment. For all auditory fear conditioning and extinction studies, animals were placed into a sound-isolating chamber and received an auditory conditioned stimulus (CS) and/or electric footshock unconditioned stimulus (US) controlled by MED-PC (MED Associates). The CS was a series of 5-kHz tone pips (1 Hz with 250 ms on and 750ms off, 20 s, 74 dB) and the US was a scrambled footshock (1 s, 0.7 mA), co-terminating with the CS unless otherwise stated. All trials were separated with variable intertrial intervals (2.5 min on average). The blue or orange light was generated by a diode-pumped solid-laser (473 or 589 nm, Shanghai Laser, 15 mW from tip of optic fiber). For all photoinhibition studies, laser illumination was initiated 400 ms before the stimulus onset and lasted until 50 ms after it ended. For optogenetic inactivation during CS or US fear conditioning, animals were conditioned with three CS-US pairings, and procedures were identical for all groups. For optogenetic inactivation during CS fear conditioning, the US was given 1 s after CS offset. For optogenetic inactivation at BLA terminals during the shock-US fear conditioning, three CS-US pairings of 0.5-mA shock intensity were used. In offset control groups, the laser was lit 50–70 s (pseudorandomly) after each trial. For optogenetic stimulation experiments during fear conditioning, blue laser pulses (10 Hz, 20-ms duration) were given with or without weak shocks (1 s, 0.3 mA). During retrieval, 24 h after conditioning, animals received five CS-alone presentations in a different context. In all extinction experiments, animals were trained with three CS-US pairings on Day 1. On Day 2, rats were presented with 22 CS without footshock in a different context. On Day 3, rats received five CS-alone presentations in the extinction context. For optogenetic inactivation during CS or during the shock omission period of extinction, the orange laser was illuminated throughout CS or 3 s from the 19th pip, respectively. For optogenetic stimulation experiments during extinction, blue laser pulses (5 Hz, 20 ms duration) were given during the CS extinction period. In pharmacological experiments, Prazosin (3 μ g/ μ l; P7791, Sigma-Aldrich) or vehicle were microinjected (0.2 μ l, 0.1 μ l/min) through internal cannula (extended 1.4 mm from guide cannula) 10 min before extinction. For Prazosin-alone experiments (**Fig. 4j**), animals used in the Prazosin + optogenetic stimulation experiment (**Fig. 4i**) were reconditioned and counterbalanced before Prazosin or vehicle injection prior to re-extinction. For optogenetic inactivation during extinction retrieval, animals received five CS presentations with laser illumination. For the c-Fos study, animals were subjected to the abovementioned fear conditioning and/or extinction protocols, except that an unpaired control group received three footshocks immediately after the start of session, followed by three CS presentation during training. All animals were killed for analysis 90 min after the end of each c-Fos experiment. ‘Fear’ was operationally defined as measurable behavioral freezing (cessation of movement) responses, which were scored either manually by an individual blind to the treatment conditions or through the use of automated freezing scoring programs (Med Associates). Automated scoring was used only for fear conditioning retrieval tests, as the behavioral boxes used for this were specifically designed for automated scoring. The use of this term is not meant to imply a conscious feeling state but rather a behavioral response that accompanies other visceral changes and occurs in response to threat. This is an important distinction prompting a potential change in the definition of ‘fear conditioning’ to ‘threat conditioning’²¹. We use the term ‘fear’ here because of its explanatory power for neuroscientists, though we acknowledge that its use is in flux.

In vivo electrophysiology. The electrode and optic fiber array was advanced 40–100 μ m daily, until we could record from light-responsive neurons. Electrodes were connected to a headstage (Neuralynx Inc.) containing 36 unity-gain operational amplifiers. Spiking activity was digitized at 40 kHz, bandpass-filtered from

300 Hz to 3 kHz and acquired through a Neuralynx data acquisition system. At the conclusion of the experiment, recording sites were verified histologically with electrolytic lesions using 15–20 s of 20-mA direct current. Offline single-unit spike sorting was performed using SpikeSort 3D (Neuralynx). Principal component scores were calculated for unsorted waveforms and plotted in a three-dimensional principal-component space. A group of waveforms were considered to be generated from a single neuron if the waveforms formed a discrete, isolated cluster in the principal-component space and did not contain any interspike intervals less than 1 ms. Typically only a single cell was recorded on each stereotrode/tetrode, and in all cases, the cells/waveforms were clearly discriminable from background multiunit activity, which was very low because we used a local reference electrode. To ensure and verify the stability of single-cell recordings, once a cell or set of cells was isolated, all experiments for that recording session were done in a single day, and the stability of recordings was assessed by verifying the similarity of waveform shapes before and after each experiment. To avoid analysis of the same neuron recorded on different channels, we computed cross-correlation histograms.

For the behavioral experiments combined with *in vivo* electrophysiology, after at least one single well-isolated light-responsive neuron was encountered, rats received five CS presentation (pre-CS). Animals were then moved to a new context and subjected to auditory fear conditioning training with 12 CS–US pairings (2-ms, 2-mA eyelid shocks at 7 Hz for 1 s, beginning 300 ms after offset of final CS pip). Starting 90 min after training, rats received 20 CS presentations during extinction training in the pre-CS context. For the overtraining experiments, rats received 12 CS–US pairings during a retraining session and were then subjected to three different conditions in the training context on the next day: (i) shocks delivered without preceding CS, (ii) shocks preceded by CS and (iii) CS without shocks. During these sessions, each condition was presented in a pseudorandom order eight times (24 trials in total). After that, electrodes were advanced until new light-responsive cells were isolated. Overtraining recording sessions and subsequent electrode advancement continued in this manner until the electrodes were no longer in the LC. For all sessions, the average intertrial interval was 2.5 min.

Electrophysiological data analyses. To determine whether units were laser responsive, the averaged firing rates in the baseline and laser periods were calculated for each trial. For baseline firing rate analyses (Supplementary Figs. 2a, b and 3), average firing rates were calculated during 20 or 60 s of activity before the first CS onset at each phase (pre-CS, training, early and late extinction). Laser responses were assessed using two-tailed paired *t* test analyses of averaged values. Perievent histograms and cumulative spikes were conducted in Matlab (MathWorks) or Neuroexplorer (NEX Technologies). For max *Z* and heat plot analyses, the PSTH of each cell was calculated by converting bin values to *z*-scores using the formula $Z_i = (S_i - \mu)/\sigma$, where μ and σ are the mean and s.d. of the prestimulus period (20 s before stimulus onset), respectively, S_i is the firing rate and i is the individual bin (S_i = firing rate for an individual bin). *Z*-score analyses were obtained from all putative NA neurons or from each light responsive neuron in Matlab. A neuron was considered to be significantly responsive to CS and/or US if there was at least one bin with $Z_i > 3$ during the CS–US period.

Histology and immunohistochemistry. To verify transgene (ArchT, eArchT3.0, GFP, tdTomato and mCherry) expression and the locations of optical fiber tips, cannulae and recording electrodes in targeted brain areas, rats were overdosed with 25% chloral hydrate and perfused with 4% paraformaldehyde in PBS. After postfixation, brains were sliced in 40- μ m (50- μ m for efferent study) coronal sections using a cryostat. Optic fiber and electrode placement, as well as virus expressions, were verified using a fluorescence microscope. Animals were excluded from the analyses if the optic fiber/electrode placement was incorrect or if virus expression did not meet the criteria (minimal expression levels or, in rare cases, where retrogradely labeled neurons were apparent outside and in close proximity to the LC).

For immunohistochemistry, free-floating sections were washed in 0.1 M PBS containing 0.3% Triton-X 100 (PBST), followed by a 30-min incubation in PBST containing 2.0% normal donkey serum (PBSTS). Sections were then incubated in the primary antibodies diluted in PBSTS for 24 h (72 h for c-Fos experiments) at

4 °C in the dark. The primary antibodies used were a rabbit anti-c-Fos (1:1,000; sc-52, Santa Cruz Biotech), mouse or rabbit anti-TH (1:2,000; MAB5280 or AB152, Millipore), mouse or rabbit anti-GFP (1:2,000; A11120 or A11122, Life Technologies Japan) and rabbit anti-RFP (1:2,000; ab62341, Abcam). After repeatedly washing with PBST, sections were incubated for 1 h at room temperature in secondary antibodies diluted in PBSTS. The secondary antibodies were Alexa Fluor 488-, 555- or 647-conjugated donkey anti-rabbit, Alexa Fluor 488-, 555- or 647-conjugated donkey anti-mouse (1:1,000; Life Technologies Japan) and (for the efferent study) Alexa Fluor 594-conjugated donkey anti-rabbit (1:200; Life Technologies Japan). After rinsing with PBST, sections were mounted onto slides and coverslipped with Fluoromount Plus (Cosmobio Co., Ltd.). For the efferent study, we used Autofluorescence Eliminator Reagent (2160, Millipore) before coverslipping to reduce background autofluorescence. Validation of all antibodies for use in rats was performed by the manufacturers and is available through individual company websites.

Confocal imaging. Sections were imaged under a confocal laser scanning microscope (FluoView FV-1000, Olympus). For the c-Fos study, counts of immunoreactive (IR) neurons for green retrobeads, red retrobeads or double-labeled for c-Fos⁺retrobead⁺ in the LC were examined by an observer blinded to the group allocations. All sections counted were 120 μ m apart throughout the anterior–posterior extent of LC, and cell counts were made for the entire LC in each section. For the efferent mapping study, synaptophysin expression was occasionally detected in cells outside the LC. To ensure that only synaptophysin-mCherry from LC neurons was quantified, animals in these cases were excluded from the analysis (3 of 8 animals, only in LA/B-projecting experiments). Images were taken from the virus-injected side using tiling and *z*-stack functions with a 20 \times objective. Binary *z*-stacked confocal images were generated and thresholded in ImageJ. The density of mCherry (number of mCherry⁺ pixels/total pixels in region of interest) was quantified for each region of interest and averaged across at least three sections. From the averaged density values and based on a previously published analytic approach⁸, calculations were made to determine fractional efferent innervation in each region of interest (for data in Figure 4d, density of each brain region/summed densities of all regions) and relative innervation values for selected regions of interests (for data in Figure 4e, f, density of selected brain region/density of injected brain region).

Statistical analysis. Data distribution was assumed to be normal, and our analytic approaches were based on previously published work^{8,18,39}, but normality was not formally tested. Statistical analyses were performed using GraphPad Prism (GraphPad Software, Inc.). Group differences were detected using one-way ANOVA, one-way repeated measures (RM) ANOVA, two-way ANOVA or two-way RM ANOVA where appropriate. Significant main effects or interactions were followed by Newman-Keuls or Bonferroni *post hoc* comparisons, as applicable. Single-variable differences were detected with two-tailed paired or unpaired Student's *t* tests. No statistical methods were used to predetermine sample sizes, but our sample sizes in electrophysiology, behavior and histology experiments are similar to or more than those reported in previous publications^{8,18,39}. All behavioral results were replicated in multiple groups/runs of the each experiment. All physiology data was replicated across multiple animals. Anatomical results were obtained from multiple animals. For all results, the significance level was set at $P < 0.05$, and significance for *post hoc* comparisons was set at $*P < 0.05$, $**P < 0.01$, $***P < 0.001$ and $****P < 0.0001$.

A Life Sciences Reporting Summary is available.

Data and code availability. The data and code that support the findings of this study are available from the corresponding authors upon reasonable request.

- Wickersham, I.R., Finke, S., Conzelmann, K.-K. & Callaway, E.M. Retrograde neuronal tracing with a deletion-mutant rabies virus. *Nat. Methods* **4**, 47–49 (2007).
- Mebatsion, T., Konig, M. & Conzelmann, K.K. Budding of rabies virus particles in the absence of the spike glycoprotein. *Cell* **84**, 941–951 (1996).
- Finke, S. & Conzelmann, K.K. Virus promoters determine interference by defective RNAs: selective amplification of mini-RNA vectors and rescue from cDNA by a 3' copy-back ambisense rabies virus. *J. Virol.* **73**, 3818–3825 (1999).

Life Sciences Reporting Summary

Nature Research wishes to improve the reproducibility of the work that we publish. This form is intended for publication with all accepted life science papers and provides structure for consistency and transparency in reporting. Every life science submission will use this form; some list items might not apply to an individual manuscript, but all fields must be completed for clarity.

For further information on the points included in this form, see [Reporting Life Sciences Research](#). For further information on Nature Research policies, including our [data availability policy](#), see [Authors & Referees](#) and the [Editorial Policy Checklist](#).

► Experimental design

1. Sample size

Describe how sample size was determined.

The number of animals in each experimental group given throughout are standard sample sizes for classical fear conditioning experiments and cell quantification experiments.

2. Data exclusions

Describe any data exclusions.

Animals were excluded if the cannula/electrode placement or virus expression wasn't satisfactory (Online Methods). For efferent mapping study, animals were excluded if fluorophore from amygdala injections was expressed in cells outside of LC (Confocal imaging section in Online Methods).

3. Replication

Describe whether the experimental findings were reliably reproduced.

All behavioral results were replicated in multiple groups/runs of the each experiment. All physiology data was replicated across multiple animals. Anatomical results were obtained from multiple animals.

4. Randomization

Describe how samples/organisms/participants were allocated into experimental groups.

A single animal was randomly selected from the colony room before each individual conditioning session.

5. Blinding

Describe whether the investigators were blinded to group allocation during data collection and/or analysis.

Experimenters were blind during behavioral scoring (Freezing response analysis) and histological evaluation (Histological verification) in Online Methods.

Note: all studies involving animals and/or human research participants must disclose whether blinding and randomization were used.

6. Statistical parameters

For all figures and tables that use statistical methods, confirm that the following items are present in relevant figure legends (or in the Methods section if additional space is needed).

n/a Confirmed

- The exact sample size (n) for each experimental group/condition, given as a discrete number and unit of measurement (animals, litters, cultures, etc.)
- A description of how samples were collected, noting whether measurements were taken from distinct samples or whether the same sample was measured repeatedly
- A statement indicating how many times each experiment was replicated
- The statistical test(s) used and whether they are one- or two-sided (note: only common tests should be described solely by name; more complex techniques should be described in the Methods section)
- A description of any assumptions or corrections, such as an adjustment for multiple comparisons
- The test results (e.g. P values) given as exact values whenever possible and with confidence intervals noted
- A clear description of statistics including central tendency (e.g. median, mean) and variation (e.g. standard deviation, interquartile range)
- Clearly defined error bars

See the web collection on [statistics for biologists](#) for further resources and guidance.

► Software

Policy information about [availability of computer code](#)

7. Software

Describe the software used to analyze the data in this study.

Freezing during fear conditioning retrieval (section on Fear conditioning and extinction) was quantified by automated scoring software (Med Associates). Electrophysiology analyses (section on Electrophysiological data analyses) were performed using a combination of Neuroexplorer and Matlab. Efferent density analyses (section on Confocal imaging) were performed with ImageJ. Statistical analyses (section on Statistical analysis) were performed with GraphPad Prism.

For manuscripts utilizing custom algorithms or software that are central to the paper but not yet described in the published literature, software must be made available to editors and reviewers upon request. We strongly encourage code deposition in a community repository (e.g. GitHub). *Nature Methods* [guidance for providing algorithms and software for publication](#) provides further information on this topic.

► Materials and reagents

Policy information about [availability of materials](#)

8. Materials availability

Indicate whether there are restrictions on availability of unique materials or if these materials are only available for distribution by a for-profit company.

All materials are available from the authors or from manufacturers (listed in Methods section)

9. Antibodies

Describe the antibodies used and how they were validated for use in the system under study (i.e. assay and species).

We described all antibodies in the Histology and Immunohistochemistry section. Validation of all antibodies for use in rats or mice was performed by the manufacturers and is available through individual company websites.

10. Eukaryotic cell lines

a. State the source of each eukaryotic cell line used.

N/A

b. Describe the method of cell line authentication used.

N/A

c. Report whether the cell lines were tested for mycoplasma contamination.

N/A

d. If any of the cell lines used are listed in the database of commonly misidentified cell lines maintained by [ICLAC](#), provide a scientific rationale for their use.

N/A

► Animals and human research participants

Policy information about [studies involving animals](#); when reporting animal research, follow the [ARRIVE guidelines](#)

11. Description of research animals

Provide details on animals and/or animal-derived materials used in the study.

We used Long Evans tyrosine hydroxylase-Cre, Long Evans rats, and C57BL6 mice

Policy information about [studies involving human research participants](#)

12. Description of human research participants

Describe the covariate-relevant population characteristics of the human research participants.

N/A